New states in ^{18}Na and ^{19}Mg observed in the two-proton decay of ^{19}Mg

I. Mukha,[1,*] L. Grigorenko,[1,2,3] L. Acosta,[4] M. A. G. Alvarez,[5] E. Casarejos,[6,7] A. Chatillon,[1] D. Cortina-Gil,[6] J. M. Espino,[5] A. Fomichev,[2] J. E. García-Ramos,[4] H. Geissel,[1] J. Gómez-Camacho,[5] J. Hofmann,[1] O. Kiselev,[1] A. Korsheninnikov,[3] N. Kurz,[1] Yu. A. Litvinov,[1] I. Martel,[4] C. Nociforo,[1] W. Ott,[1] M. Pfützner,[1,8] C. Rodríguez-Tajes,[6,9] E. Roeckl,[1] C. Scheidenberger,[1] M. Stanoiu,[1,10] K. Sümmerer,[1] H. Weick,[1] and P. J. Woods[11]

[1]*GSI Helmholtzzentrum für Schwerionenforschung, D-64291 Darmstadt, Germany*
[2]*Joint Institute for Nuclear Research, RU-141980 Dubna, Russia*
[3]*RRC "Kurchatov Institute," RU-123184 Moscow, Russia*
[4]*Department of Applied Physics, University of Huelva, E-21071 Huelva, Spain*
[5]*University of Seville, E-41012 Seville, Spain*
[6]*University of Santiago de Compostela, E-15782 Santiago de Compostela, Spain*
[7]*University of Vigo, E-36310 Vigo, Spain*
[8]*Faculty of Physics, University of Warsaw, PL-00681 Warszawa, Poland*
[9]*GANIL, CEA/DSM-CNRS/IN2P3, BP 55027-14076 Caen Cedex 05, France*
[10]*IFIN-HH, Post Office Box MG-6, Bucharest, Romania*
[11]*University of Edinburgh, EH1 1HT Edinburgh, United Kingdom*

(Received 7 February 2012; revised manuscript received 5 April 2012; published 30 April 2012)

Previously unknown states in ^{18}Na and ^{19}Mg have been studied by measuring the trajectories of their decay products with microstrip detectors. Analyzing angular correlations of the fragments provided information on decay energies and widths of the parent states. The ground state of ^{18}Na has been detected and its one-proton decay energy of 1.23(15) MeV determined. Four previously unknown states in ^{19}Mg at 2.1, 2.9, 3.6, and 5.2 MeV have been observed. The competition between simultaneous and sequential two-proton emission of states in ^{19}Mg is discussed, and the conclusion of a direct mechanism of $2p$ radioactivity of the ^{19}Mg ground state is confirmed.

DOI: 10.1103/PhysRevC.85.044325 PACS number(s): 21.10.−k, 21.45.−v, 23.50.+z, 27.20.+n

I. INTRODUCTION

Two-proton ($2p$) radioactivity, or the spontaneous decay of an atomic nucleus by $2p$ emission, has revealed unexpectedly long half-lives for all $2p$ precursors investigated so far: ^{45}Fe [1], ^{48}Ni [2], ^{54}Zn [3], ^{19}Mg [4], and ^{94m}Ag [5]. The regular occurrence of long-lived $2p$ precursors has been explained by a quantum-mechanical theory which describes $2p$ radioactivity on the basis of a three-body model [6] as simultaneous (or direct) $2p$ emission through large centrifugal three-body and Coulomb barriers. Experimental data on ^{19}Mg [4] were obtained using an experimental technique to investigate decays of proton-unbound nuclei with lifetimes from 10^{-9} to 10^{-12} s, as proposed by Mukha and Schrieder [7]. The trajectories of all decay products were tracked with microstrip detectors, making it possible to deduce their decay vertices as well as their angular correlations. Observation of ^{19}Mg and its $2p$ radioactivity as well as proton-proton correlations from $2p$ decays of ^{19}Mg were reported [4,8]. All experimental data have been reproduced quantitatively by the three-body model, considering ^{19}Mg as a $p + p + {}^{17}$Ne system that decays by simultaneous $2p$ emission.

In addition to the direct $2p$ decay of the ^{19}Mg ground state (g.s.), sequential emission of protons from excited states in ^{19}Mg via intermediate states in ^{18}Na, a two-body subsystem of ^{19}Mg, is possible. To understand this mechanism quantitatively, information on the lowest states in ^{18}Na is required. The first data on ^{18}Na states were ambiguous, allowing the g.s. to be located either 0.42(17) or 1.27(17) MeV above the proton-decay threshold [9]. Recently, the spectroscopic properties of the unbound isotope ^{18}Na were studied by the resonant-elastic-scattering reaction $p + {}^{17}$Ne [10]. Four excited states in ^{18}Na were identified while its g.s. remained undetected. The authors of Ref. [10] also proposed an explanation for the half-life value of the ^{19}Mg g.s. in terms of sequential emission of protons via tails of broad excited states in ^{18}Na.

In the present article, we extend the analysis of the proton-^{17}Ne correlations from our ^{19}Mg experiment [4,8]. In contrast to the previous works [9,10], we find unambiguous evidence for the identification of the g.s. of ^{18}Na. We report also newly observed excited states in ^{19}Mg, whose $1p$ decays populate states in ^{18}Na. The derived level schemes and decay branches are sketched in Fig. 1. We discuss the interplay of simultaneous and sequential $2p$ decays of the ^{19}Mg states and argue in favor of direct $2p$ emission from the ^{19}Mg g.s. and sequential $2p$ emission from the excited states of ^{19}Mg.

II. EXPERIMENT

In our experiment, a beam of ^{20}Mg was produced by fragmentation of ^{24}Mg at the projectile-fragment separator (FRS) [11] with an average intensity of 400 ions s^{-1} and an energy of 450 A MeV. Nuclei of ^{19}Mg were produced by

*I.Mukha@gsi.de

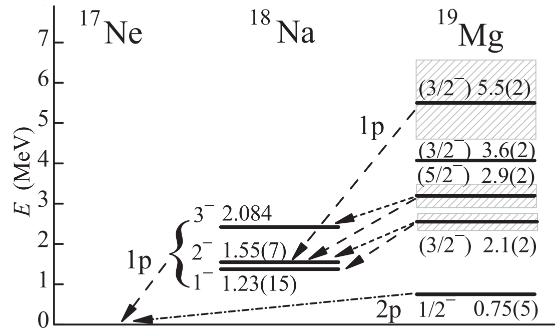

FIG. 1. The observed states in ^{19}Mg and ^{18}Na whose energies (in MeV) are shown relative to the respective $1p$ and $2p$ thresholds. The main and the minor $^{19}\text{Mg} \rightarrow {}^{18}\text{Na} + p$ branches are indicated by dashed and dotted arrows, respectively. The spins and parities given in parentheses are tentative assignments. The energy of ^{18}Na(3^-) is taken from Ref. [10].

secondary fragmentation of ^{20}Mg on a 2 g/cm^2 thick ^{9}Be target positioned in the midplane of the FRS. A sketch of the detectors near the latter target is presented in Fig. 1 of Ref. [12]. A silicon detector array was positioned downstream of the target. It consisted of four large-area microstrip detectors that measured positions of coincident hits of two protons and a heavy ion (HI). This allowed the reconstruction of all fragment trajectories as well as deriving the coordinates of the corresponding reaction vertex and the angular p-p and p-HI correlations with an angular resolution of 1 mrad. The experimental setup and the data-analysis procedures were recently presented in detail (see Ref. [12]). In particular, we have shown how identification of $2p$-precursor states and their decay energies and widths can be obtained from analyzing angular correlations of the decay products. The known properties of four states in ^{15}F, ^{16}Ne, and ^{19}Na were reproduced. Below we re-evaluate our data on direct and sequential decays of ^{19}Mg.

III. EXPERIMENTAL RESULTS

The identification of the ^{19}Mg g.s. and the measurement of its $2p$ decay energy were performed by analyzing angular correlations of protons with respect to ^{17}Ne. Such angular correlations are similar to transverse momentum correlations which are normally used to identify nuclear states and their decay channels [12]. We assumed that all measured channels feed only the g.s. of ^{17}Ne (i.e., no evidence for excitations of the 1.288-MeV state in ^{17}Ne which de-excites by γ-ray emission was found). In the top panels of Figs. 2(a) and 2(b), simultaneous and sequential $2p$ decays are shown schematically while the bottom panel illustrates the respective momentum correlations as obtained in our experiment. The $2p$ decays of narrow states are arranged along arcs with radius $\rho = \sqrt{\theta^2_{p1\text{-Ne}} + \theta^2_{p2\text{-Ne}}} =$ const, since two protons share the same total decay energy. This feature can be used to select certain $2p$-precursor states, as we have previously demonstrated on $2p$ decays of the known states in ^{16}Ne [12].

The measured angular correlations $\theta(p_1\text{-}^{17}\text{Ne})$-$\theta(p_2\text{-}^{17}\text{Ne})$ shown in Fig. 2(c) display several distinct clusters of events that apparently resemble the schemes displayed in Figs. 2(a) and 2(b). In our previous work [4] the small-angle events around $\theta(p\text{-}^{17}\text{Ne}) = 30$ mrad were attributed to the ^{19}Mg g.s., while those at larger angles, above 45 mrad, were tentatively ascribed to a single excited state in ^{19}Mg with a $2p$-decay energy of 3.2 MeV. We argue below that the most intense groups may be assigned to sequential $1p$ decays of four excited states in ^{19}Mg via low-lying states in ^{18}Na, including, in particular, its g.s.

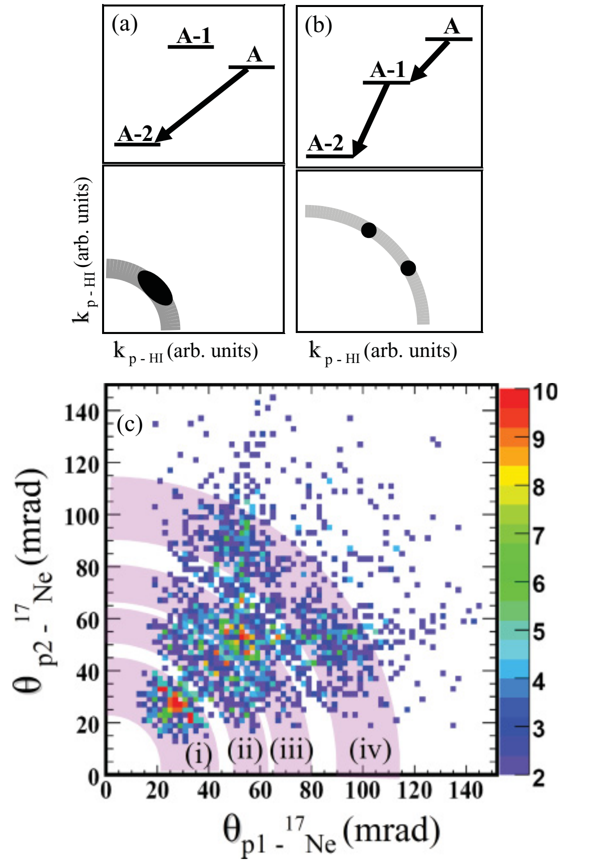

FIG. 2. (Color online) Schematic drawing of transverse momentum correlations $k_{p1\text{-HI}}$-$k_{p2\text{-HI}}$ in panels (a), (b) expected for two alternative mechanisms of $2p$ decay (illustrated in the respective top panels) from a parent nucleus A to a daughter nucleus A-2: (a) direct three-body decay or simultaneous $2p$ emission, (b) sequential emission of protons via a narrow intermediate state in nucleus A-1. (c) Measured angular (p_1-^{17}Ne)-(p_2-^{17}Ne) correlations (color boxes with scale shown on the right-hand side). The shadowed arc areas (i–iv) (along $\rho =$ const) indicate locations of simultaneous or sequential $2p$ decays of the most intensively populated states in ^{19}Mg.

In the first step of the data analysis, we consider angular correlations obtained by gating on angular p_2-^{17}Ne slices in a way similar to that of Ref. [4]. Figure 3 shows the p_1-^{17}Ne correlations obtained by restricting $\theta_{p2\text{-Ne}}$ as indicated on top of each spectrum. The un-gated distribution displayed in Fig. 3(a) shows two intense peaks around 30 and 55 mrad, which we interpret as being due to the "g.s." and "excited state(s)" ("ex.s."). Figure 3(b) shows the p_1-^{17}Ne correlations corresponding to the lowest g.s. peak in the other pair p_2-^{17}Ne. The contribution from the g.s. peak dominates, whereas the ex.s. peak is suppressed, in contrast to the ungated distribution

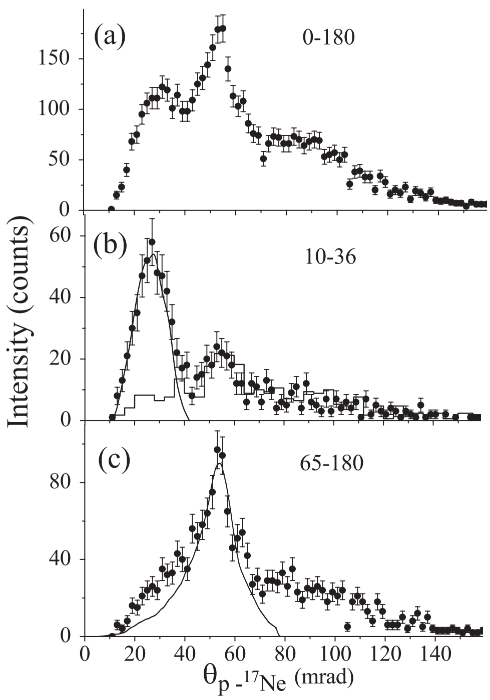

FIG. 3. (a) Angular p_1-^{17}Ne correlations (solid circles with statistical uncertainties) obtained from the measured ^{17}Ne + p + p data shown in Fig. 2(c) without imposing any gate condition. (b) Angular p_1-^{17}Ne distribution obtained from the same data by selecting the other proton angle, $\theta_{p2\text{-Ne}}$, within the range from 10 to 36 mrad, which corresponds to the assumed g.s. of ^{19}Mg. The solid curve represents the Monte Carlo simulation of the detector response to $^{19}\mathrm{Mg}_{\mathrm{g.s.}} \rightarrow {}^{17}\mathrm{Ne} + p + p$ with a 2p-decay energy of 0.75(5) MeV. The histogram represents the assumed background deduced from the data for a $\theta_{p2\text{-Ne}}$ gate from 110 to 180 mrad; it contributes 15% to the peak at angles from 10 to 36 mrad. (c) Angular p_1-^{17}Ne distribution projected by choosing the $\theta_{p2\text{-Ne}}$ gate from 65 to 180 mrad. The solid line is the simulation of the final-state interaction of protons with ^{17}Ne due to the 1.55-MeV resonance in ^{18}Na.

displayed in Fig. 3(a). Therefore, the g.s. and ex.s. peaks cannot be explained by emission of protons from one and the same state in ^{19}Mg because in this case both peak integrals should be equal. Moreover, the ex.s. decay always occurs when the second proton is emitted under a large angle with respect to ^{17}Ne [see Fig. 3(c)], which is equivalent to large excitations in ^{19}Mg. The qualitative explanation of this behavior is that the "excited state" peak is due to a ^{18}Na resonance occurring in the p_1-^{17}Ne pair.

The experimental data are compared to Monte Carlo simulations, assuming two decay mechanisms: (i) simultaneous or direct 2p decay $^{19}\mathrm{Mg} \rightarrow {}^{17}\mathrm{Ne} + p + p$ according to the predictions of the three-body model [13] and (ii) sequential emission of protons from ^{19}Mg via one of the low-lying ^{18}Na levels identified in [10]. In both cases, the 2p-decay energies were obtained by fitting the peaks in the experimental spectra. The peak around 30 mrad in Fig. 3(b) is described by the direct 2p decay with $Q_{2p} = 0.75(5)$ MeV. The peak around 55 mrad in Fig. 3(c) can be interpreted as sequential emission of protons from continuum excited states in ^{19}Mg ($9 < Q_{2p} < 15$ MeV) to a single narrow ^{18}Na state which decays by emission of a 1.5-MeV proton. The latter assumption is based on final-state interaction of protons with ^{17}Ne and is justified by the newly identified 2^- resonance in ^{18}Na at 1.55 MeV [10]. As can be seen from Fig. 3(c), the whole spectrum is not described by assuming a single ^{18}Na state, and further analysis of the exclusive data is needed.

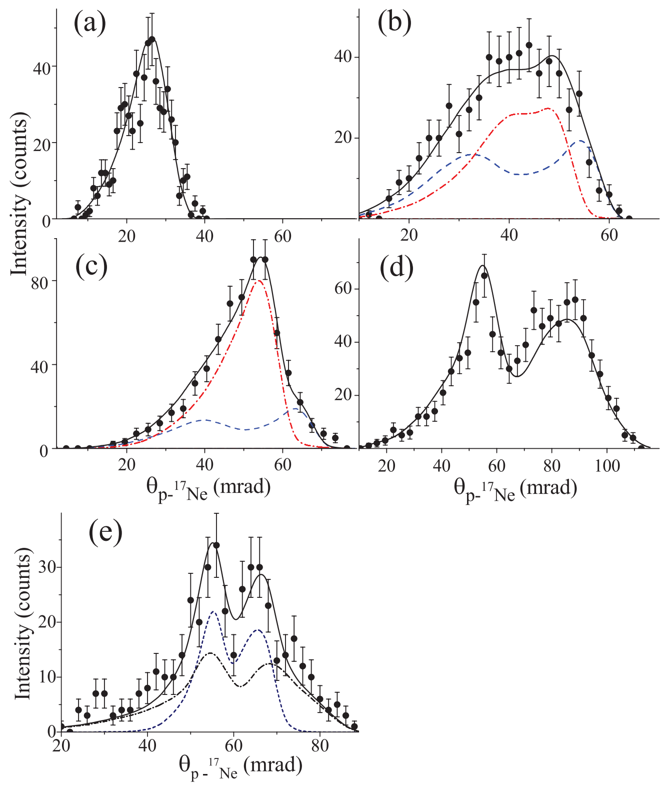

FIG. 4. (Color online) Angular p-^{17}Ne correlations (solid circles with statistical uncertainties) selected from the ^{17}Ne + p + p data by choosing the arc gates (i–iv) shown in Fig. 2(c). (a) The 2p decay of the ^{19}Mg g.s. selected by gate (i), that is, the condition $20 < \rho < 45$ mrad. The solid curve shows the best-fit simulation of the three-body model using a 2p-decay energy of $Q_{2p} = 0.76(6)$ MeV. (b) The 2p decay of the ^{19}Mg "first-excited" state selected by the gate (ii), $50 < \rho < 65$ mrad. The solid curve displays the simulation of the sequential 2p decay of the state at 2.14 MeV via two intermediate states in ^{18}Na, the g.s. at $Q_{1p} = 1.23$ MeV (dash-dotted line), and the 2^- state at 1.55 MeV (dashed line). (c) The 2p decay of the "second-excited" state in ^{19}Mg selected by gate (iii), $65 < \rho < 80$ mrad. The solid line is the best-fit simulation of the sequential 2p decay of the ^{19}Mg state at 2.9 MeV via the 2^- and 3^- states in ^{18}Na (the dash-dotted and dashed curve, respectively). (d) The 2p decay of the suggested high-lying state in ^{19}Mg at $Q_{2p} = 5.5$ MeV selected by gate (iv), $90 < \rho < 115$ mrad. The solid curve represents the best-fit simulation of the decay of this state by sequential 1p emission via $^{18}\mathrm{Na}^*(2^-)$. (e) Angular p-^{17}Ne correlations selected by choosing the arc gate between areas (iii) and (iv) shown in Fig. 2(c), that is, the condition $80 < \rho < 90$ mrad. The dashed curve shows the simulation of the sequential 2p decay of the suggested excited state in ^{19}Mg via $^{18}\mathrm{Na}^*(2^-)$, with the fitted values $Q_{2p} = 3.6(2)$ MeV and $\Gamma < 0.2$ MeV. The dash-dotted curve represents the contribution due to the 2p decay of the neighboring ^{19}Mg state at $Q_{2p} = 5.5$ MeV. The solid curve is the sum fit.

TABLE I. Nuclear levels observed in this work, listed according to isotope, tentative spin-parity J^π assignment, decay channel, $1p/2p$ decay energy Q^{exp}, and width Γ^{exp} (the latter two given in MeV).

Isotope	J^π	Decay	Q^{exp}	Γ^{exp}	Reference
^{18}Na	$(1)^-$	$^{17}\mathrm{Ne}+p$	1.23(15)	<0.2	This work
^{18}Na	?	$^{17}\mathrm{Ne}+p$	1.27(17)	0.54(13)	[9]
^{18}Na	2^-	$^{17}\mathrm{Ne}+p$	1.55(7)	$0.25(^{-15}_{+25})$	This work
^{18}Na	2^-	$^{17}\mathrm{Ne}+p$	1.552(5)	0.005(3)	[10]
^{19}Mg	$1/2^-$	$^{17}\mathrm{Ne}+p+p$	0.76(6)	1.14×10^{-10}	This work
^{19}Mg	$(3/2^-)$	$^{17}\mathrm{Ne}+p+p$	2.14(23)	0.4(2)	This work
^{19}Mg	$(5/2^-)$	$^{17}\mathrm{Ne}+p+p$	2.9(2)	$0.6(^{-4}_{+6})$	This work
^{19}Mg	$(3/2^-)$	$^{17}\mathrm{Ne}+p+p$	3.6(2)	<0.2	This work
^{19}Mg	$(3/2^-)$	$^{17}\mathrm{Ne}+p+p$	5.5(2)	2.0(8)	This work

The second step of the data analysis considers angular p-^{17}Ne correlations obtained by selecting arc gates along $\rho=$ const. This method is similar to that applied to ^{16}Ne [12]. The chosen gates are shown in Fig. 2(c). The angular p-^{17}Ne correlation displayed in Fig. 4(a) corresponds to a selection by the lowest arc gate (i), which picks out the g.s. of ^{19}Mg. Under this condition, one observes exclusively the peak due to the g.s. of ^{19}Mg, while the background component is reduced dramatically in comparison with Fig. 3(b). The peak fit performed by assuming the direct $2p$ decay of the ^{19}Mg g.s. and neglecting the background contribution yields $Q_{2p}=0.76(6)$ MeV.

The angular p-^{17}Ne correlations shown in Figs. 4(b), 4(c), and 4(d) were obtained by imposing the larger-arc gates (ii), (iii), and (iv) indicated in Fig. 2(c). They correspond to $2p$ decays of three excited states in ^{19}Mg. Indications on these intensively populated levels can be observed in Fig. 2(c). The two cases which are easiest to interpret are marked by arc areas (iii) and (iv). In both cases the corresponding p-^{17}Ne correlations show pronounced peaks which we interpret as signatures for $2p$ decays from a single state in ^{19}Mg. In both spectra displayed in Figs. 4(c) and 4(d), one of the peaks occurs at the same p-^{17}Ne angle of 55 mrad, which makes sense only for sequential emissions of protons via the same resonance in ^{18}Na. These spectra were fitted by assuming decays $^{19}\mathrm{Mg}^*\rightarrow{}^{18}\mathrm{Na}+p\rightarrow{}^{17}\mathrm{Ne}+p+p$ with four fit parameters corresponding to $Q_{2p}(^{19}\mathrm{Mg}^*)$, $\Gamma(^{19}\mathrm{Mg}^*)$ and $Q_{1p}(^{18}\mathrm{Na})$, $\Gamma(^{18}\mathrm{Na})$. The parameters obtained in both cases for the ^{18}Na resonance are $Q_{1p}=1.55(7)$ MeV and $\Gamma=0.25(^{-15}_{+25})$ MeV, which match the 2^- state at 1.55 MeV [10]. For a quantitative reproduction of the spectrum shown in Fig. 4(c), an additional branch (about 25%) via the known 3^- state at 2.084 MeV [10] has to be postulated. The properties of the respective parent states in ^{19}Mg at 2.9 and 5.5 MeV are given in rows 7 and 9 of Table I. Evidence for one more excited state in ^{19}Mg can be seen in Fig. 2(c), where there are peaks indicated in the area $80<\rho<90$ mrad, between gates (iii) and (iv). Figure 4(e) presents the angular correlations selected correspondingly. For a quantitative reproduction of the data, two components are needed. The first one is the sequential $2p$ decay of the above-mentioned broad 5.5-MeV state via $^{18}\mathrm{Na}(2^-)$, whose low-energy tail describes about half of the spectrum. To account for the rest of data, the sequential $2p$ decay of an additional state in ^{19}Mg via $^{18}\mathrm{Na}(2^-)$ has to be involved. It should be very narrow and is located at $Q_{2p}=3.6(2)$ MeV, as shown in row 8 of Table I.

Evidence in favor of the ^{18}Na g.s. was obtained in the decay of the lowest-lying excited state in ^{19}Mg, which is indicated in Fig. 2(c) by arc area (ii). Though these events are not very well separated from the neighboring ones marked by arc (iii), the respective $2p$-decay patterns are distinctively different, which can be seen by comparing the respective p-^{17}Ne correlations shown in Figs. 4(b) and 4(c). The distribution from the $2p$ decay of the "first-excited state" of ^{19}Mg [Fig. 4(b)] is much broader and does not show any indication of the 1.5-MeV peak which is present in the "second-excited state" $2p$ decay spectrum in Fig. 4(c). Such a structure cannot be explained by sequential $2p$ decay via any previously known state in ^{18}Na. Thus, the existence of a new level in ^{18}Na has to be suggested. Its properties were derived by fitting the p-^{17}Ne correlations shown in Fig. 4(b), assuming sequential $2p$ decay of an unknown state in ^{19}Mg via an unknown intermediate state in ^{18}Na. The parameters of the ^{18}Na resonance derived from a four-parameter fit are listed in row 1 of Table I together with the properties (in row 6) of the respective parent state in ^{19}Mg at 2.14 MeV. An additional $2p$ decay branch via the 2^- state in ^{18}Na is needed to describe the correlations in Fig. 4(b) quantitatively; its relative weight is 35%. The inferred $1p$-decay energy of 1.23(15) MeV is slightly lower than the value of 1.3 MeV preliminarily deduced in our previous publication [4] and is close to the 1.27(17)-MeV assignment of the ^{18}Na g.s. suggested tentatively in the invariant-mass measurements [9]. The corresponding mass excess of the ^{18}Na g.s. is therefore 25.02(15) MeV. We note that there is no evidence in our spectra for the other $1p$ peak at $Q_{1p}=0.42(16)$ MeV proposed in Ref. [9]. The difference between the experimentally measured mass of ^{18}Na and the corresponding mass predicted by using charge conjugation of its mirror state in ^{18}N (on the basis of charge-symmetric mass relationships [14]) is $\Delta M(Z,N)=-395(150)$ keV, which matches reasonably the systematics of proton-unstable nuclei where the average value $\overline{\Delta M(Z,N)}=-577(325)$ keV displays a general shift of the Thomas-Ehrman type [14].

IV. DISCUSSION

The theoretical predictions of the g.s. mass and low-lying structure of ^{18}Na are ambiguous. Both shell-model [10,15] and relativistic mean-field calculations [16] predict the lowest 0^-, 1^-, and 2^- states to be unbound with decay energies of $\sim$1.5 MeV. However, they have quite different sets of spectroscopic factors within a configuration space of a proton in the $1d_{5/2}$ shell coupled to ^{17}Ne, which itself is a mixture of $(sd)^2$ and $[(sd)^2(1p)^{-1}]$ configurations. The two lowest 1^- and 2^- states were predicted to be separated by about 200 keV. In Ref. [10], the 2^- state in ^{18}Na was identified at 1.552(5) MeV leaving 1^- as the only possible assignment for the g.s. of ^{18}Na. Its width was predicted to be 22 keV [10], which is consistent with the upper limit of 200 keV determined in our work.

The information obtained on ^{18}Na [10] can be used for assigning tentative J^π values to the newly observed ^{19}Mg levels. In particular, the measured width of 0.4 MeV for the 2.14 MeV state in ^{19}Mg and its decay branches agree only with an assignment of $J^\pi = 3/2^-$ because it preferably decays by emitting a proton with an angular momentum of $\ell_p = 0$ to the 1^- and 2^- states in ^{18}Na. The corresponding upper-limit estimate (Wigner limit) for the partial proton width yields about 0.1–0.3 MeV. All other spin parities would correspond to $\ell_p > 0$ and result in much smaller Wigner limits. Similar considerations lead to the $5/2^-$ assignment for the 2.9-MeV state in ^{19}Mg because it decays predominantly to the 2^- and 3^- states in ^{18}Na but not to its 1^- state. A comparison of the mirror nuclei ^{19}N and ^{19}Mg also supports the $3/2^-$ and $5/2^-$ assignments for the 2.14- and 2.9-MeV states in ^{19}Mg, respectively: The first two excited $3/2^-$ and $5/2^-$ states in ^{19}N are at excitation energies of 1.141 and 1.676 MeV, respectively [17]. We suggest that these levels arise from the coupling of a $p_{1/2}$ neutron hole to the first 2^+ state of the ^{20}Mg core, in analogy to the conclusion drawn for the (tentative) mirror states in ^{19}N [17]. We note that the possible intense $5/2^-$ excitation of ^{19}Mg is a surprising result for reactions of one-neutron knockout from ^{20}Mg where neutrons are mostly in $p_{1/2}$ and $p_{3/2}$ configurations; this requires further studies. The high-lying excited state in ^{19}Mg at 5.5 MeV emits a proton to ^{18}Na(2^+) with the Wigner-limit estimates for its width of 4.6, 2.8, and 0.85 MeV for ℓ_p of 0, 1, and 2, respectively. This excludes d-wave proton emission, which leaves tentative J^π of $1/2^+$, $3/2^-$, $5/2^-$, $7/2^+$, for the 5.5-MeV state.

We compared the observed excitations in ^{19}Mg with shell-model calculations. As we have observed only the ^{19}Mg states which are most-intensively populated in one-neutron removal reactions from ^{20}Mg projectiles, configurations of those states are likely to have large overlaps with the ^{20}Mg g.s. In particular, one-neutron removal from $p_{1/2}$ and $p_{3/2}$ shells can populate $1/2^-$ and $3/2^-$ states in ^{19}Mg, respectively. We calculated the respective spectroscopic factors in the $spsdpf$-shell space with the WBP interaction of Warburton-Brown [18] using the NUSHELL@MSU code [19], and the results are summarized in Table II. From Table II one can see that the g.s. and three excited states of ^{19}Mg are populated strongly. The properties of the first excited state $3/2^-$ in ^{19}Mg, its decay energy and decay branches are reproduced well though the theory does not agree with the data at higher energies, and further investigations are needed.

As a final topic, we want to address the question if the observation of broad resonances in ^{18}Na [10] requires reinterpreting the direct (three-body) character of the $2p$ decay of the ^{19}Mg g.s. Assie *et al.* [10] suggest that the ^{19}Mg g.s. decays sequentially via the tails of the broad intermediate resonances in ^{18}Na at 1.84 MeV ($J^\pi = 0^-$, $\Gamma = 0.3$ MeV) and 2.03 MeV ($J^\pi = 1^-$, $\Gamma = 0.9$ MeV). The essential condition for the sequential-decay mechanism is that the first-emitted proton and the intermediate ^{18}Na state are separated in space before the subsequent decay of this state occurs. Otherwise, the ^{19}Mg decay should be treated as simultaneous $2p$ emission or direct three-body decay. Goldansky [20] has suggested as a criterion for the direct decay that $Q_{2p} + \Gamma_r/2 < E_r$, where E_r and Γ_r are the energy and the width of the intermediate resonance, respectively. This is clearly fulfilled in our case. The same conclusion was reached in a recent review where the competition between simultaneous and sequential $2p$ decay was investigated (see Chap. VII.C.3 in [21]): Any resonance in ^{19}Mg below $Q_{2p} = 1.5$ MeV should decay by direct $2p$ emission.

TABLE II. Nuclear levels in ^{19}Mg most intensively populated in one-neutron knock-out from ^{20}Mg projectiles according to shell-model calculations. The ^{19}Mg states are listed according to spin parity J^π, spectroscopic factor C^2S of overlap $\langle ^{19}\mathrm{Mg} \mid ^{20}\mathrm{Mg}\rangle$, calculated $2p$-decay energy Q_{2p}^{SM} (given in MeV), and partial width Γ_i (given in MeV) of a $2p$-decay branch i via the J_i^π state in ^{18}Na.

J^π	C^2S	Q_{2p}^{SM}	Γ_i	^{18}Na(J_i^π)
$1/2^-$	2.18	0.76[a]	–	–
$3/2_1^-$	0.57	2.44	0.186	1^-
			0.054	2^-
$3/2_2^-$	0.38	4.35	0.25	1^-
			0.02	2^-
$3/2_3^-$	0.35	5.21	large	$1^-, 2^-$
			0.134	1_2^-
			0.030	2_2^-
			0.028	3^-

[a]The $2p$ decay energies of the ^{19}Mg states are normalized to the experimental value of the ^{19}Mg g.s.

To illustrate further the interplay between sequential and direct $2p$-decay mechanisms, we have performed more calculations within the above-mentioned three-body model for $2p$ decays of the ^{19}Mg g.s., which includes both direct and sequential emission mechanisms [22]. For simplicity, we assume only one intermediate resonance in the $p + {}^{17}$Ne subsystem. We calculate proton-energy distributions in terms of the parameter $\varepsilon \sim E_p/E_T$, which describes how the two protons share the total decay energy E_T (for a fixed value of E_r).

Figure 5(a) shows our results for the case that the intermediate resonance represents a state in ^{18}Na with $J^\pi = 1^-$ at $E_r = 1.23$ MeV, with a narrow width $\Gamma_r = 0.1$ MeV. At low energies, the decay protons share the total energy E_T in a broad region always centered around $\varepsilon = 0.5$, which is a typical feature of the simultaneous (direct) $2p$ decay. A sequential decay should manifest itself in the observation that the energy of one proton peaks near and below 1.23 MeV. Such a feature is not present in Fig. 5(a). However, at $E_T \simeq 1.2 \cdot E_r$ one can see a dramatic change of the proton-energy distributions which are

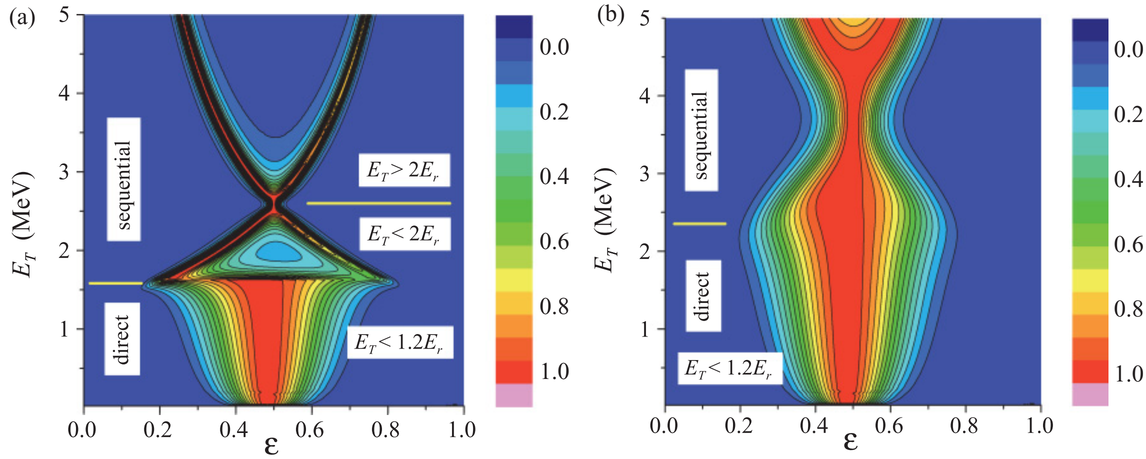

FIG. 5. (Color online) Intensity distributions of $2p$ decays from ^{19}Mg (arbitrary yields corresponding to the color scale shown on the right-hand side) as a function of the total $2p$-decay energy E_T and the parameter $\varepsilon \sim E_p/E_T$. The distributions are calculated with a three-body model assuming a single resonance in the intermediate nucleus ^{18}Na with energy E_r and width Γ_r. (a) Decays by taking into account the g.s. of ^{18}Na at $E_r = 1.23$ MeV with $\Gamma_r = 0.1$ MeV. (b) Decays via the 1_2^- state in ^{18}Na at $E_r = 2.03$ MeV, $\Gamma_r = 0.9$ MeV [10].

characterized by two distinct and intense peaks corresponding to sequential $2p$ emission via the ^{18}Na state. With increasing E_T, the 1.23-MeV peak represents a decreasing fraction of E_T; that is, its position moves along the right narrow ridge toward the left-hand side. The first-emitted proton peak moves complementarily toward the right-hand side. At $E_T \simeq 2 \cdot E_r$, the proton energies are equal, which is a special case of undistinguishable decay channels. Such a situation requires a separate detailed consideration elsewhere.

In Fig. 5(b), we display a similar distribution where now the intermediate resonance in ^{18}Na is assumed to be a broad state ($\Gamma_r = 0.9$ MeV) at $E_r = 2.03$ MeV, in accordance with the results of Ref. [10]. Though the detailed structure of the distribution is washed out (due to the large width of the intermediate state), one can recognize a general trend similar to the previous case, with two regions corresponding to direct and sequential decays. We conclude from these schematic calculations that in the case of the ^{19}Mg g.s., where $E_T \ll E_r$, the direct $2p$-emission mechanism dominates while the observed excited states decay sequentially via ^{18}Na.

In summary, the unbound g.s. of ^{18}Na and three new excited states in ^{19}Mg have been deduced from the measured angular correlations of their decay products. The data yielded the decay energies and widths of these states. Schematic model calculations support the direct three-body decay mechanism for the g.s. and sequential proton emission for the excited states of ^{19}Mg.

ACKNOWLEDGMENTS

The authors are grateful to N. K. Timofeyuk for the shell-model calculations and constructive discussions of the data. This work has been supported by Contract EURONS No. EC-I3, FPA2006-13807-C02-01 MEC, and FPA2009-08848 MICINN (Spain). L.V.G. is supported by the FAIR-Russia Research Center by Grants RFBR No. 08-02-00892 and RFBR No. 11-02-00657, Russian Ministry of Industry and Science Grant No. NSh-7235.2010.2, and by the LOEWE program of the State of Hessen (HIC for FAIR), Germany.

[1] K. Miernik *et al.*, Phys. Rev. Lett. **99**, 192501 (2007).
[2] M. Pomorski *et al.*, Phys. Rev. C **83**, 061303 (2011).
[3] B. Blank *et al.*, Phys. Rev. Lett. **94**, 232501 (2005).
[4] I. Mukha *et al.*, Phys. Rev. Lett. **99**, 182501 (2007).
[5] I. Mukha *et al.*, Nature (London) **439**, 298 (2006).
[6] L. V. Grigorenko, R. C. Johnson, I. G. Mukha, I. J. Thompson, and M. V. Zhukov, Phys. Rev. Lett. **85**, 22 (2000).
[7] I. Mukha and G. Schrieder, Nucl. Phys. A **690**, 280c (2001).
[8] I. Mukha *et al.*, Phys. Rev. C **77**, 061303(R) (2008).
[9] T. Zerguerras *et al.*, Eur. Phys. J. A **20**, 389 (2004).
[10] M. Assié *et al.*, AIP Conf. Proc. **1409**, 93 (2011).
[11] H. Geissel *et al.*, Nucl. Instrum. Methods Phys. Res., Sect. B **70**, 286 (1992).
[12] I. Mukha *et al.*, Phys. Rev. C **82**, 054315 (2010).
[13] L. V. Grigorenko, I. G. Mukha, and M. V. Zhukov, Nucl. Phys. A **713**, 372 (2003); **740**, 401(E) (2004).
[14] E. Comay, I. Kelson, and A. Zidon, Phys. Lett. B **210**, 31 (1988).
[15] H. T. Fortune, R. Sherr, and B. A. Brown, Phys. Rev. C **73**, 064310 (2006).
[16] L. S. Geng, H. Toki, A. Ozawa, and J. Meng, Nucl. Phys. A **730**, 80 (2004).
[17] D. Sohler *et al.*, Phys. Rev. C **77**, 044303 (2008).
[18] B. A. Brown, Prog. Part. Nucl. Phys. **47**, 517 (2001).
[19] B. A. Brown and W. D. M. Rae, NUSHELL@MSU, MSU-NSCL Report, 2007 (unpublished).
[20] V. I. Goldansky, Nucl. Phys. **19**, 482 (1960).
[21] M. Pfützner, L. V. Grigorenko, M. Karny, and K. Riisager, arXiv:1111.0482v1 [nucl-ex] [Rev. Mod. Phys. (in print)].
[22] L. V. Grigorenko, I. A. Egorova, M. V. Zhukov, R. J. Charity, and K. Miernik, Phys. Rev. C **82**, 014615 (2010).